Turbulent Mixing in Shear Driven Stratified Fluid

Amrita Shravat

January 12, 2009

1 Introduction

Background turbulence frequently causes mixing across gravitationally stable density interfaces in atmosphere and ocean. Some common examples include turbulence by surface winds or the cooling causing the deepening of the upper ocean mixed layer into stably stratified pycnocline and turbulent mixing at the tropopause causing the growth of a planetary boundary layer. There can be some mixing at the thermocline due to discharge of the buoyant jets from power plants. These mixing processes are important in order to understand and control the biological activities and dispersion of pollutants in the environment ([3]). For example, the diffusion of methane gas in mine shafts.

Many laboratory and associated theoretical studies have considered the response of a stratified fluid to impulsive surface forcing. [3] provides an excellent review on studies with turbulence and vertical shear, investigating the growth of mixed layer in a stratified fluid. The nature of mixing at sheared and shear free density interfaces is very different. For example, the mixing in shear-driven stratified flows, where a well mixed turbulent layer entrains an adjacent non-turbulent layer, is believed to depend upon the external forcing, the depth of the mixed layer and the buoyancy jump across the layer. All these parameters are investigated in the present study of 2-layer fluid system.

The first set of experiments undertaken to explore the growth of the mixed layer as a function of these factors were that of [4]. They found that the entrainment rate was proportional to the friction velocity u_* ($(= |\tau|/\rho_0)^{1/2}$, where τ is the surface shear stress and ρ_0 is the reference density) and Ri_τ^{-1}, where Ri_τ is the overall Richardson number, defined as $g'h/u_*^2$. The current investigation has been motivated by the stratified flow experiments of [2] and [1] in cylindrical geometries. The present work is based on the earlier two-layer model of [1], where a horizontal disk at the base of the tank drives the flow. Their analysis showed that for Richardson Number, $Ri_B(= g'h/\Omega^2R^2) < 1.5$, the growth of the elevation of the interface separating the upper (almost quiescent) layer of constant density from the lower mixed region is proportional to Ri_B^{-1}. Note that h is the depth of the mixed layer, Ω is the rotation rate of the disk and R is the radius of the disk. The buoyancy is defined as $g' = g(\rho_L - \rho_u)/\bar{\rho}_L$, where g is the gravitational acceleration, ρ_L is the density of the lower layer fluid, ρ_u is the density of the fluid in the upper layer and $\bar{\rho}_L$ is the average density of the fluid in the lower layer, relevant if the fluid in the lower layer is linearly stratified.

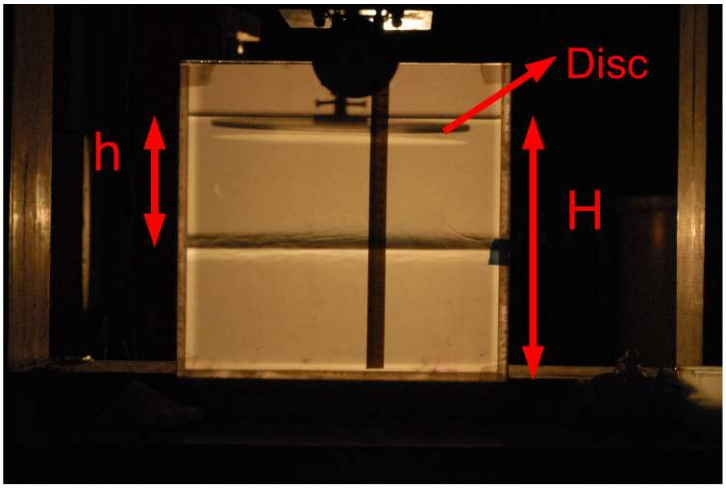

Figure 1: Experimental set-up showing a tank with a horizontal disk spinning the fluid in the upper layer.

The experiments in the current work are characterised by the growth of a mixed layer, separated by the undisturbed stratified lower fluid by a curved surface. In this report, the experimental set-up is discussed, along with the dimensionless parameters that come into play. The experimental results are presented and an attempt to offer a theoretical explanation of these results is made.

2 Experimental set-up and parameters

The experiment comprises of a cylindrical tank of diameter 30cm, with a horizontal disk at the top attached to a motor. Figure (1) and figure (2) show a square tank used initially. The disk is just below the free surface of the top layer, fully immersed in the upper layer fluid. The radius of the disk is 12 cm. The rate of rotation of the disk is controlled by a motor. The rotation rate ranges from $1s^{-1} \leq 2\pi\Omega \leq 12s^{-1}$, where Ω is the angular rotation rate, which remains constant during an experiment. As the disk spins, it provides energy for mixing the two layers. A conductivity probe is used to obtain vertical density profiles in the fluid. The total depth of the fluid, $H = 27$cm is fixed and is the same for every experiment. The depth of the upper layer, h, varies during the experiments. The initial depth of the upper layer is indicated as $h_0 = h(t = 0)$, and the depth during an experiment is $h = h(t)$. For most experiments, h_0 is varied between 6cm and 20.6cm. The consequences of changing the Richardson number by varying R, the radius of the disk, are not explored in the present experiments.

The most important dimensionless parameter for the flow is the Richardson number ([1]). The following are the definitions of the Richardson number that will be used throughout this report.

$$Ri_B(t) = \frac{g'h}{\Omega^2 R^2},$$

where R is the radius of the disk, $g' = g(\rho_L - \rho_u)/\bar{\rho}_L$ (ρ_L, ρ_u and $\bar{\rho}_L$ as defined in the previous section), and Ω is the rate of rotation of the disk. Ri_B is constant for most part of the experiment as can be seen from Figure 6. For almost all the experiments, after an initial spin-up (when the fluid in the top layer is set into motion), Ri_B reaches a constant value and maintains that value until the very end of the experiment, where the cylinder bottom affects the experiment. Near the bottom, the boundary layer effects cannot be neglected. Consequently, the value of Ri_B used is this work is $\bar{Ri}_B$, i.e the average value of Ri_B calculated ignoring the beginning and the end of an experiment. It should be noted that in this definition, the velocity is assumed to be the"solid body rotation" velocity, i.e. u_u (see below) is given by ΩR. Hence, Ri_B is the same as Ri_τ, discussed in previous section, if the velocity is ΩR.

$$Ri_0 = \frac{g_0' h_0}{\Omega^2 R^2},$$

where g_0' is the initial buoyancy jump across the interface between the upper and lower layer, measured before starting the experiment and h_0 is the initial depth of the upper layer.

$$Ri_u = \frac{g' h}{u_u^2} = Ri_B \left(\frac{\Omega^2 R^2}{u_u^2} \right), \quad \text{where } u_u \text{ is the characteristic velocity in the upper layer.}$$

$$Ri_m = \frac{g' L_m}{u_u^2},$$

where , L_m is the interfacial length scale (i.e. radius of an eddy at the interface). L_m is proportional to the Ozmidov scale, L_0. The Reynolds number in the present experiments is sufficiently high for the flow to be regarded as turbulent. Hence, allowing for the assumption that the flow is independent of Reynolds number. The Schmidt number, Sc (ratio of kinematic viscosity to mass transfer diffusion coefficient), is not an important parameter for the flow as $Sc \gg 1$ for a salt stratified water solution and it is constant for all the experiments. Thus, the overall fluid motion and mixing process is assumed to depend on a single parameter, the Richardson number.

2.1 A Typical Experiment

Figure 2 shows a two-layer experiment, with $\bar{Ri}_B = 0.56$. The upper layer is well mixed with fluid being pulled up by the spinning disk, resulting in a dome-shaped interface. The Ekman layer, below the disk, causes the fluid below to rise up. This results in a circulation, where the fluid ascends from the middle and comes down from the side of the tank. As the mixing at the interface occurs, the upper layer deepens until all the fluid in the lower layer is mixed. It is worth noting that the lower layer is very quiescent. It is motionless and retains this property until it is completely mixed. A schematic of the fluid circulation in the upper and lower layer is shown in figure 3. The overturning billows seen at the interface (for the case where $Ri_0 \leq 1$), entrain the lower layer fluid. This mechanism converts the kinetic energy (provided by the disk) of the fluid in the upper layer, into potential energy by lifting up the denser fluid particles from the lower layer and mixing them with the rest of

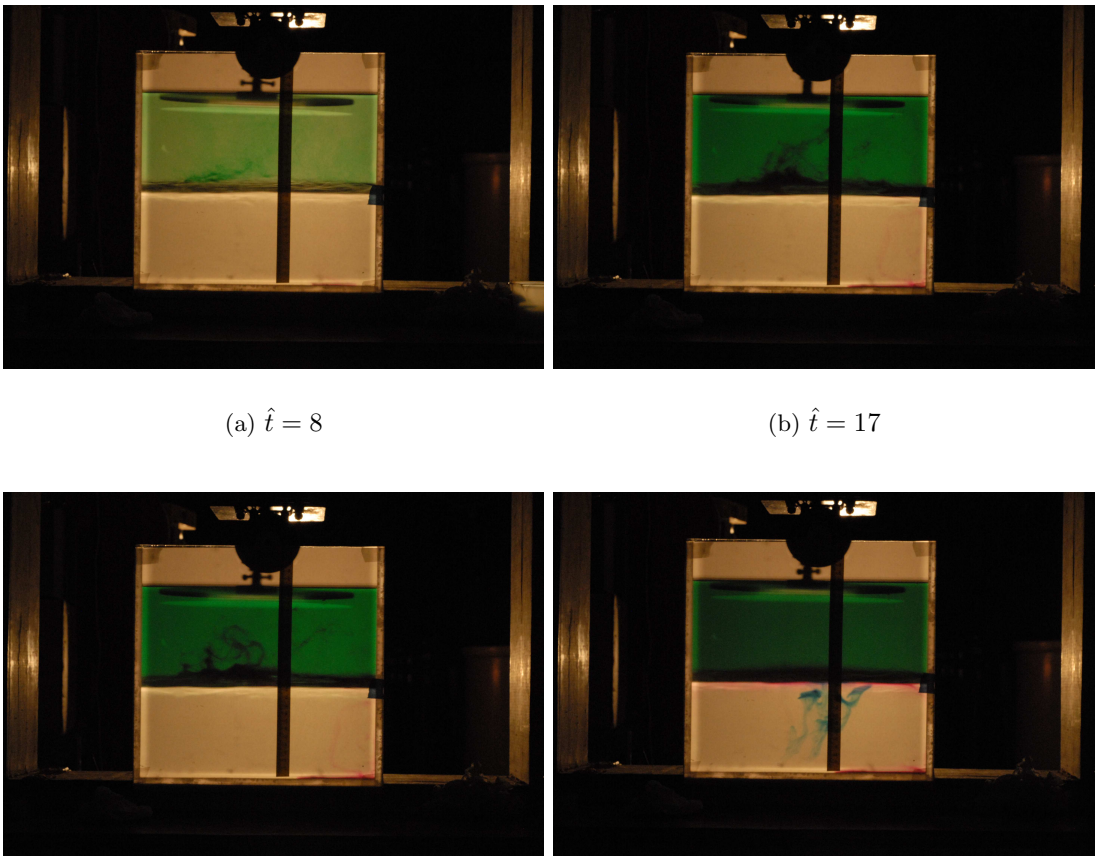

(a) $\hat{t} = 8$ (b) $\hat{t} = 17$

(c) $\hat{t} = 18$ (d) $\hat{t} = 28$

Figure 2: A two-layer experiment with $\Omega = 1s^{-1}, \hat{t} = \Omega t$, $R\bar{i}_B = 0.56$. In figure 2(c), the fluid in the upper layer is pulled by the disk, spinning at the rate Ω at the top. The fluid in the lower layer is motionless. The dye is rising in 2(d) because it is lighter than the lower layer fluid.

the fluid in the upper layer. It is the size of these overturning billows (in terms of L_m) that determines the rate at which the fluid is mixed. However, once the size exceeds a certain critical value, these billows can no longer develop and the fluid is not mixed efficiently. For $Ri_0 > 1$, a completely different regime is observed. The flow is no longer turbulent and the overturning billows are replaced by waves at the interface.

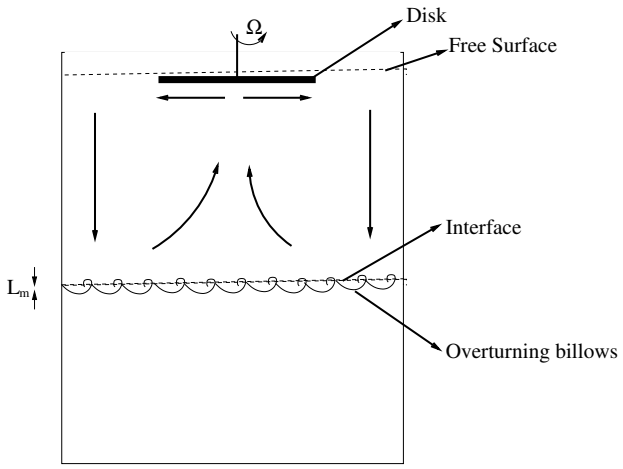

Figure 3: A schematic of the flow in the cylindrical tank, with the disk spinning at the top. There is no circulation in the lower layer fluid.

As mentioned earlier, a conductivity probe is used to obtain vertical profiles of the fluid's density. Figure 4, shows one such profile with $\bar{Ri}_B = 0.19$. The height of the interface (in mm) is plotted against the density of the fluid (in g/cm^3). The evolution in time of the profiles is from left to right. The profile on the extreme left represents the initial density of the two layers. After the disk starts spinning, the first density profile obtained is the second profile from the left (blue line). It is clear, from looking at the profiles from left to right, that the upper layer is deepening as the level of the interface is going down in each subsequent profile. As expected, the lower layer maintains its density until it is completely mixed with the upper layer fluid.

3 Experiments

The following table shows the various experiments conducted to observe the mixing in a two-layer stratified fluid.

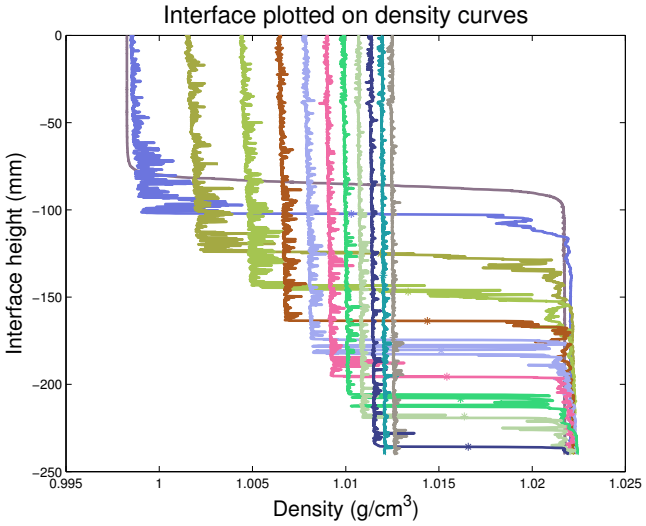

Figure 4: A typical vertical profile of the density during an experiment with $\bar{Ri}_B = 0.19$. The evolution of the profiles in time is from left to right.

Experiment	Ri_0	h_0 (cm)	$\Omega(s^{-1})$	$g_0'(cms^{-2})$	$\bar{Ri}_B$
080713lo40	0.1527	8.7	3	22.7407	0.19
080714lo40	0.3109	17.8	3	22.6470	0.32
080715lo40	0.2367	13.5	3	22.7215	0.255
080716lo40	0.2554	18.5	3	17.8929	0.275
080718lo30	0.2406	6.1	2	22.7218	0.265
080720lo64	0.2336	13.5	5.4	73.1874	0.258
080721lo60	0.0851	13.5	5	22.7028	0.096
080727lo20	2.1293	13.5	1	22.7124	2.1
080731lo30	0.5317	13.5	2	22.6842	0.56
080809lo50	0.1328	13.5	4	22.6561	0.154
080810lo28	1.0016	20.6	1.8	22.6842	0.935
080812lo40	0.2124	13.5	3	20.3892	0.24

The last experiment, '080812lo40', has a buoyant upper layer and a linearly stratified lower layer with density profile evolving in time as shown in figure 5. The range of Richardson numbers explored in the experiments is shown in figure 6.

As expected, mass is conserved in all the experiments. This is clear from figure 7. The value of $Ri_B/Ri_0 = g'h/g_0'h_0$ is approximately 1 for the experiments, implying that $g'h$ is a constant. The fluctuations seen in figure 7 are due to the fact that the flow is turbulent. It is for this reason that the value of Ri_B/Ri_0 is not exactly 1. Another observation that can be made from this figure is that the value of Ri_B/Ri_0 decreases dramatically for some cases but not for the others. This can be attributed to the fact that all the profiles are included in these experiments as there were relatively few of them. Since Ri_0 for these experiments is small, the mixing takes place very quickly as there is a small density difference between the two layers. As mentioned earlier, the value of Ri_B/Ri_0 at the bottom cannot be trusted

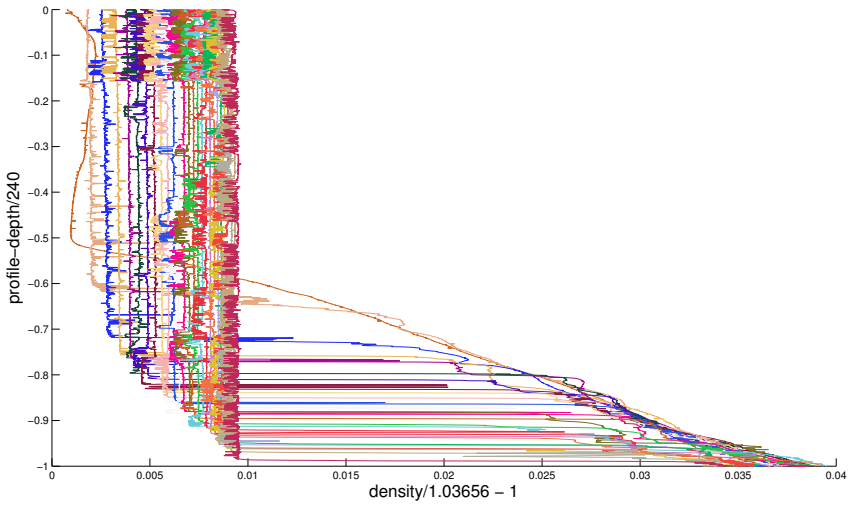

Figure 5: Density Profiles from experiment '080812lo40': Plot of density (non-dimensional) against depth that has been profiled (non-dimensional). Note the profiling depth is not the same as the total depth, $H = 27cm$, instead the profiling depth is $24cm$. Profiles evolve in time from left to right. $\bar{Ri}_B = 0.24$.

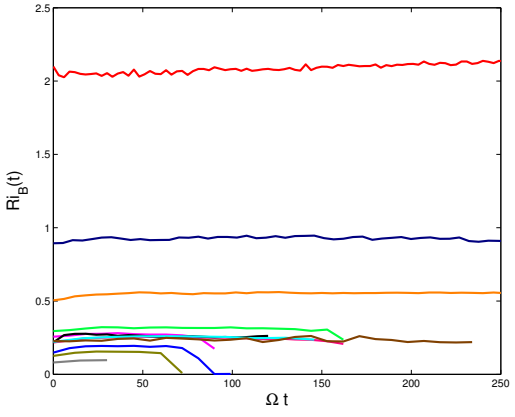

Figure 6: Range of $Ri_B(t)$ explored in the experiments.

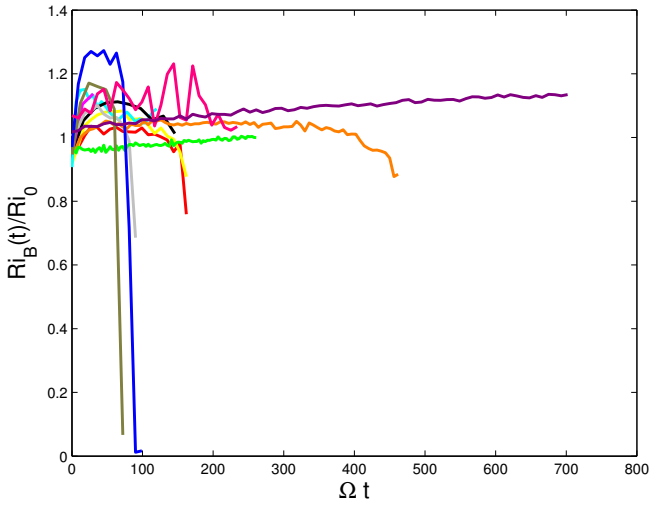

Figure 7: The value of $Ri_B(t)/Ri_0 = g'h/g'_0h_0 \sim 1$. This suggests that $g'h$ is a constant.

because of the effect of bottom boundary layer. Hence, the last few profiles show such a dramatic change in the value of $Ri_B(t)$. Moreover, the initial value for almost all the experiments is 1. It changes after the initial spin-up of the fluid, again reinforcing that after the initial spin-up period, the value of Ri_B is almost a constant. From now onwards, it is this value, found by averaging the value of $Ri_B(t)$ (excluding the beginning and the end profiles) that will be used for Ri_B.

It can be established from the following theoretical consideration that $g'h$ is a constant. If A is the cross-sectional area of the cylinder, H is the total height, h is the height of the upper layer, which evolves in time $h = h(t)$, and Q = entrainment flux, then

$$\frac{d}{dt}(Ah) = Q. \tag{1}$$

The amount of fluid entrained is

$$\frac{d}{dt}\left(A\int_0^h \rho_u\, dz\right) = Q\rho_L, \tag{2}$$

where ρ_L is the density in the lower layer. The average density in the upper layer is

$$\bar{\rho_u} = \frac{1}{h}\int_0^h \rho_u\, dz, \tag{3}$$

Hence, on substituting (3) into (2),

$$\frac{d}{dt}(Ah\bar{\rho}_u) = Q\rho_L. \tag{4}$$

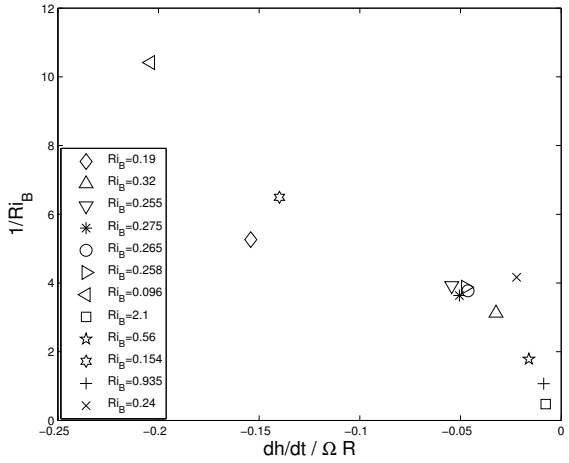

Figure 8: Plot of $dh/dt/\Omega R$ against $1/Ri_B$. The growth of the interface is not perfectly proportional to $1/Ri_B$.

which gives

$$\frac{d}{dt}[A(\bar{\rho_u} - \rho_L)h] + \rho_L \frac{d}{dt}[Ah] = Q\rho_L, \tag{5}$$

$$\frac{d}{dt}[A(\bar{\rho_u} - \rho_L)h] = 0, \tag{6}$$

$$\frac{d}{dt}[Ag\frac{(\bar{\rho}_u - \rho_L)}{\rho_L}h] = 0, \tag{7}$$

This shows that $\frac{d}{dt}(g'h) = 0$ and thus $g'h$ is a constant and mass is conserved.

In figure 8, the growth of the interface (scaled by ΩR) is plotted against $1/Ri_B$. This figure suggests that the mixing, or the growth of the interface, does not scale perfectly with Ri_B^{-1}. From the experimental results presented here, it is clear that the outcome of this work does not support the conclusion of [1], where they found that the growth of the interface is proportional to Ri_B^{-1}, where the velocity ($= \Omega R$) of the upper layer fluid is constant in each experiment. Thus the simple mixing law, inferred by [1] needs a modification. This indicates that the results do not support the assumption that the fluid is in solid body rotation, i.e. the velocity does not scale as ΩR as assumed in the definition of Ri_B. Hence, it is not completely accurate to assume that the velocity in the upper layer is the same as ΩR and that it does not change during the experiment. An immediate consequence of this result will be to re-examine the velocity of the upper layer fluid.

4 Theory

The driving disk sets up a characteristic velocity u_u in the upper layer. Assuming that the bottom layer is stationary, the interfacial stress, τ can be described by the following expression,

$$\tau = c_D \rho_L u_u^2,$$

where c_D is the drag coefficient. Hence, the work done, W, can be expressed as

$$\frac{dW}{dt} = \pi R^2 u_u \tau = \pi R^2 c_D \rho_L u_u^3, \tag{8}$$

The potential energy, PE is

$$PE = \pi R^2 \left[-g \int_0^h \rho_u z \, dz - g \int_h^H \rho_L z \, dz \right] = (\pi R^2 \rho_L) \frac{g' h^2}{2} + k, \tag{9}$$

It should be noted here that k is a constant. However, the reference level for potential energy can always be chosen such that this constant k is zero. The potential energy is negative because $z = 0$ is defined at the top of the tank. The rate of change of potential energy of the fluid parcels is proportional to the amount of power provided by the disk, i.e.

$$\frac{d}{dt} PE = \Gamma \frac{dW}{dt}, \tag{10}$$

where Γ is the flux coefficient ([5]). Assuming that $g'h$ is a constant (see previous section), this leads to

$$\frac{d}{dt} \left[(g'h)(\pi R^2 \rho_L) \frac{h}{2} \right] = \Gamma \pi R^2 c_D \rho_L u_u^3. \tag{11}$$

Hence, the interface grows as

$$\frac{dh}{dt} = 2\Gamma \frac{c_D u_u^3}{g'h}., \tag{12}$$

Let

$$\hat{h} = \frac{h}{h_0} \, , \, \hat{t} = \Omega t,$$

$$\frac{d\hat{h}}{d\hat{t}} = \frac{2 c_D \Gamma u_u^3}{\Omega h_0 g' h}. \tag{13}$$

It is quite intuitive to expect that the growth of the interface depends on the amount of energy that is spent on mixing the two layers together. The following 3 sub-sections quantify this statement based on the amount of energy (provided by the disk) that is spent on entrainment.

4.1 Case 1

Solid Body Rotation:

If none of the energy is spent on entrainment, then all of the energy provided by the disk is exhausted in moving the fluid in the upper layer. The upper layer in this case moves with a constant speed, ΩR, provided by the disk. In this case, the upper layer fluid is in solid body rotation, i.e.

$$u_u = \Omega R,$$

where u_u is the speed of the upper layer fluid.

$$\frac{d\hat{h}}{d\hat{t}} = \frac{R}{h_0}\frac{c_1}{Ri_B} = \text{constant}, \tag{14}$$

$$c_1 = 2c_D\Gamma, \tag{15}$$

$$\hat{h} - 1 = \frac{R}{h_0}\frac{c_1}{Ri_B}\hat{t}. \tag{16}$$

This case is similar to the outcome of [1], with $\frac{d\hat{h}}{d\hat{t}}$ a constant.

4.2 Case 2

ALL Energy spent on entrainment:

Assume u_u can be expressed as

$$u_u = \Omega R\left(\frac{h_0}{h}\right)^{\alpha},$$

where h_0 is the initial depth of the upper layer measured before starting the experiment. This expression means that the velocity of the upper layer fluid decreases with time. It is no longer a constant, which is the case if some energy is spent on mixing the two layers. The total kinetic energy, KE_u in the upper layer is

$$KE_u = \frac{\pi R^2}{2}\rho_{ref}u_u^2 h, \tag{17}$$

where ρ_{ref} is the density taken at some reference level. This reference density can, for example, be the average upper layer density. It is assumed that in this case all the energy is spent on mixing. This signifies that the kinetic energy of the upper layer does not change as all the energy that the disk provides is lost in mixing the two layers. Hence,

$$\frac{d}{dt}KE_u = 0,$$

Thus,

$$\frac{\pi R^2}{2}\rho_{ref}u_u^2 h = \text{constant}, \tag{18}$$

By appealing to the Boussinesq approximation, changes in ρ_{ref} can be ignored. Thus, $u_u^2 h$ is constant if $\alpha = 0.5$ i.e

$$u_u = \Omega R \left(\frac{h_0}{h}\right)^{1/2}.$$

Hence, for the above expression to hold true, the fluid must spend all the kinetic energy on mixing.

4.3 Case 3

Intermediate Case:

The two cases mentioned above are the extreme cases when either all the energy from the disk is spent on mixing or all of it is expended on spinning the fluid in the upper layer. A more sensible scenario is if part of the energy from the disk is consumed by the mixing process and part of it is spent on mobilising the fluid. Suppose, as before,

$$u_u = \Omega R \left(\frac{h_0}{h}\right)^{\alpha}.$$

Substituting this expression into equation (13) and integrating yields the following expression for $\hat{h}$:

$$\hat{h} - 1 = \left[\frac{R}{h_0}\frac{(1+3\alpha)c_1}{Ri_B}\hat{t} + 1\right]^{1/(1+3\alpha)} - 1. \tag{19}$$

Thus we can summarise the above results as follows:

- If $\alpha = 0$: Entrainment has no effect on energy - this is the case when stratification is weak.
- If $\alpha = 0.5$: All the kinetic energy from the disk is spent on entraining the lower layer fluid. Hence, there can be three dynamical regimes based on the value of Ri_B. When Ri_B is small, it can be expected that the fluid is more or less in solid body rotation. When the Richardson number is small, it is relatively easy for the upper fluid parcels to lift the lower fluid and mix. This means that more energy is left for mobilising the upper layer fluid. When Ri_B is large, it is presumed that most of the energy would be spent on lifting up the lower layer fluid. For moderate values of Ri_B, some of the energy is spent on the potential energy of the lower layer fluid parcels and a part is spent on mobilising fluid in the upper layer. This is easier to visualise from figure 9. In the three regimes shown, the velocity at the beginning is ΩR. Ri_B increases from left to right in the figure, where (a) shows that the velocity of the fluid in the upper layer is a constant as for small Ri_B most of the energy is spent on mobilising the upper layer fluid. The middle picture, (b) represents the intermediate case where the velocity is not a constant and the third case, (c) represents the large Ri_B regime. The flow in this regime is not as turbulent as the other cases. There are no overturning billows at the interface, instead it has waves. In this case, almost all the energy is exhausted in mixing the fluid layers rather than providing kinetic energy to the upper

layer fluid. The rate of change of interface drops from left to right. As expected, when stratification is weak, it is relatively easy to mix the two fluids together. However, as the stratification increases, it becomes increasingly expensive to mix the fluid. In the high Richardson number case, the mixing is very inefficient, because of the lack of overturning billows. Hence, it takes a significantly long time for the two layers to mix.

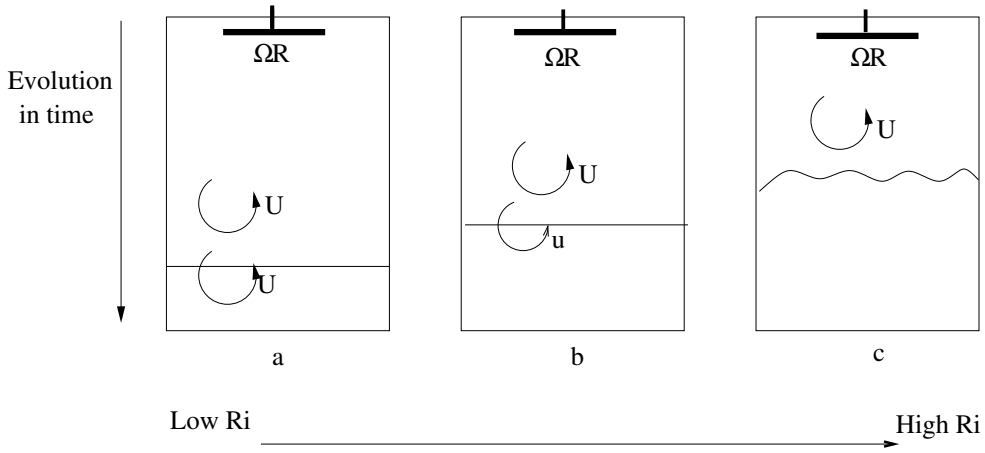

Figure 9: A sketch of the three dynamical regimes based on the Richardson number (see text). The Richardson number increases from left to right in the figure. In b, $u < U < \Omega R$ as part of the energy is spent on mixing the fluid and only part of it is used to mobilise the upper layer fluid.

5 Discussion

In order to analyse the data to test the three regimes scenario that have been discussed qualitatively, equation (19) is plotted for various values of α, with $\hat{h} - 1$ against $\hat{t}$. The constant c_1 is calculated from the initial data gathered just after the spin-up stage. It is assumed that just after the spin-up, the upper layer fluid is in solid body rotation. This is a reasonable assumption because at the beginning the work is done mainly on mobilising the upper layer fluid. The initial data (excluding the spin-up stage) is used to plot equation (16). A value of c_1 can be found from the slope of this curve. This constant c_1 is assumed constant throughout the experiment. The value of c_1 is employed to plot $\alpha = 0.2, 0.4$ and 0.5 curves. The data in figure 10 is very close to the line $\alpha = 0$, as expected from the energy arguments. The stratification in these experiments is quite weak, which suggests that the mixing requires very little energy and most of the kinetic energy from the disk is consumed by the fluid in the upper layer.

Similarly, for the curves in figure 11, the data lies above the line $\alpha = 0.5$, indicative of an intermediate regime. Figure 11(e), shows a good agreement with the theoretical arguments. The data lies just above the $\alpha = 0.5$ curve, again indicating that the upper layer fluid is

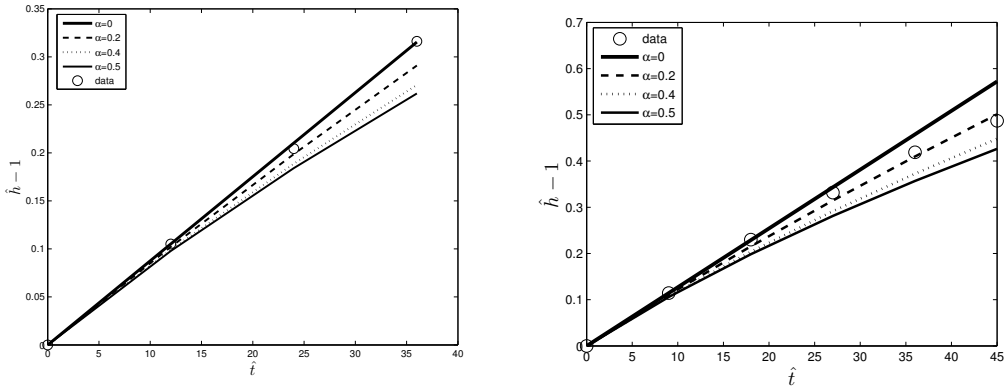

(a) $Ri_B = 0.15, c_1 = -0.0020$ (b) $Ri_B = 0.19, c_1 = -0.0030$

Figure 10: Equation (19) plotted with $\hat{h} - 1$ against $\hat{t}$. It is plotted for $\alpha = 0, 0.2, 0.4, 0.5$.

not in solid body rotation and the velocity decreases in time. For this moderate value of Richardson number, relatively more energy is required to mix the two layers. As a result, lesser energy is spent on driving the upper layer fluid. In figure 11(f), the data is very close to $\alpha = 0.5$ curve, indicating that most of the energy is consumed by the process of mixing.

Figure 12 shows the plot of $\hat{h} - 1$ against $\hat{t}$ from equation (19) for an experiment with two-layers, where the lower layer is linearly stratified. Figure 5 shows its vertical density profiles. It appears from figure 12 that the data does not fit the theoretical model. It should be noted, however, that the constant c_1 needs to be recalculated after every profile. This has not been done yet. Qualitatively, it can be seen that at the beginning, when g' is very small, the data is close to the $\alpha = 0$ curve. As g' increases, it gets closer to the $\alpha = 0.5$ line, as expected. This is consistent with the argument that the larger the value of Ri_B or stronger the stratification, the harder it is for the upper layer fluid to mix the denser lower layer. Consequently, most of the energy is spent on mixing the fluids.

The flux coefficient, Γ, (defined in section 4) can be divided into 3 components: Γ_u: mobilising flux coefficient, Γ_D: dissipation flux coefficient, Γ_ρ: Potential Energy flux coefficient. Thus, Γ_u determines the amount of energy from the disk going into mobilising the fluid in the upper layer, Γ_D determines the energy spent on dissipation and Γ_ρ, the energy that is used up in lifting the fluid parcels from below. The reason for dividing Γ into three components is to understand and establish the fraction of energy extracted from the disk to drive the upper layer fluid, mix the two layers together and dissipate.

The growth of the interface occurs due to entraining of the lower layer fluid. Thus, equation (12) can be written more precisely in terms of Γ_ρ as

$$\frac{dh}{dt} = 2\Gamma_\rho c_D \frac{u_u^3}{g'h}, \tag{20}$$

$$\frac{dh}{dt} = \frac{2\Gamma_\rho c_D}{Ri_m}\frac{L_m}{h}u_u, \;\; L_m = Ri_m\frac{u_u^2}{g'}, \tag{21}$$

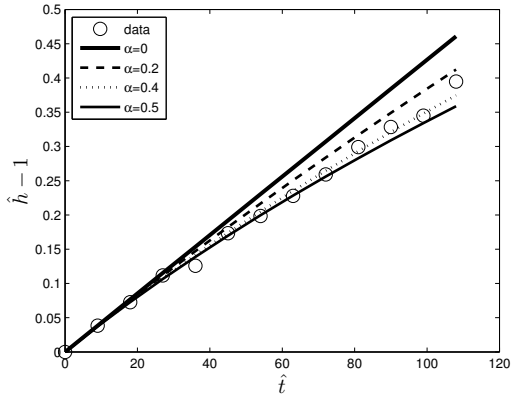

(a) $Ri_B = 0.255, c_1 = -0.0015$

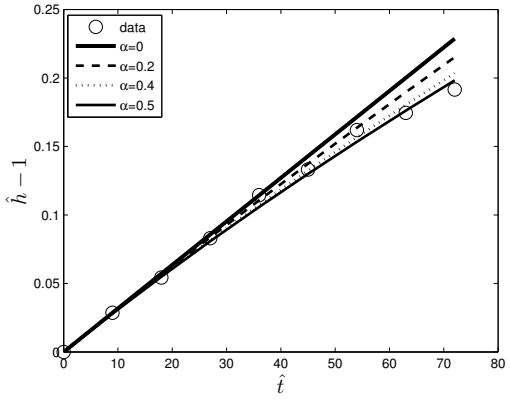

(b) $Ri_B = 0.275, c_1 = -0.0015$

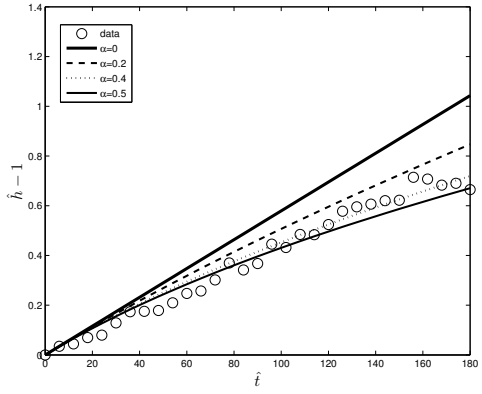

(c) $Ri_B = 0.265, c_1 = -0.0017$

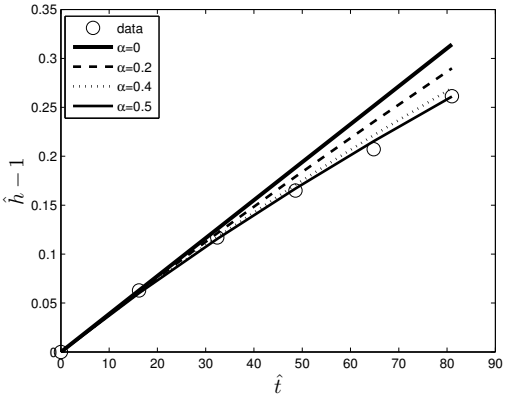

(d) $Ri_B = 0.258, c_1 = -0.0013$

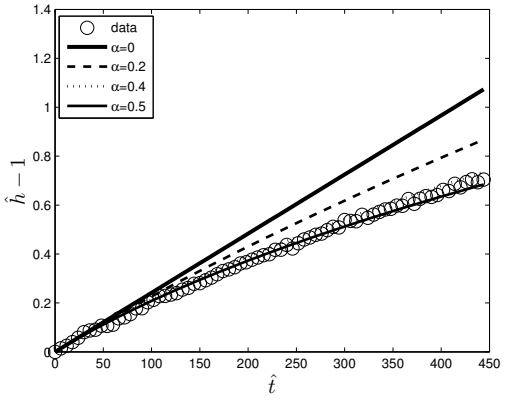

(e) $Ri_B = 0.56, c_1 = -0.0015$

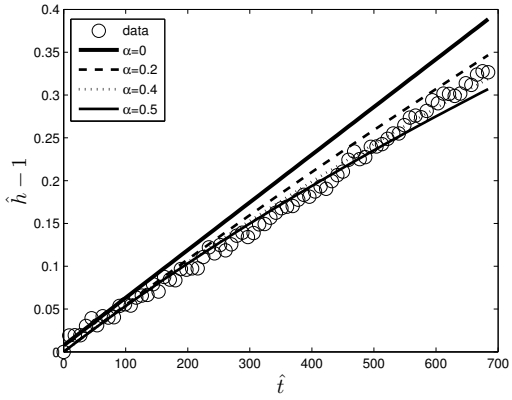

(f) $Ri_B = 0.935, c_1 = -0.00086$

Figure 11: Plot of $\hat{h}-1$ against $\hat{t}$ with value of α ranging from 0 to 0.5. The data lies above $\alpha = 0.5$ curve, suggesting that these experiments fall under the intermediate regime.

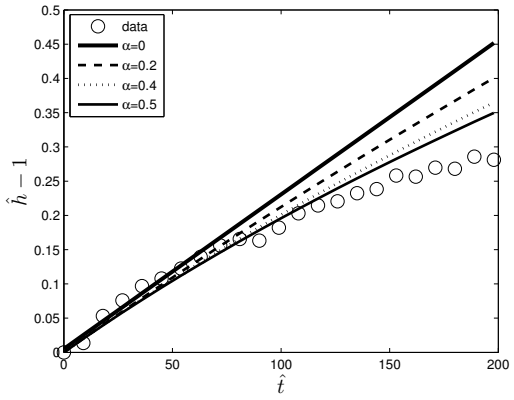

Figure 12: Linear Stratification, $Ri = 0.24, c_1 = -0.00082$

Remember L_m is the interfacial length scale. From the definition of c_1, given by (15), it seems reasonable that it should be defined more precisely as $c_1 = 2c_D\Gamma_u$, since it is the mobilising component of flux that plays an important role here. As discussed before, the kinetic energy provided by the rotating disk is spent on dissipation, increasing the kinetic energy of the upper layer by mobilising it and increasing the potential energy of the flow by lifting the heavier lower layer particles and mixing them with the upper layer. Since the flow has high Re,

$$\epsilon = \frac{a_2 u_u^3}{h}$$

(from classical turbulence theory)
Parametrizing the change in kinetic energy of the two-layer fluid by ϵ, produces the following equation

$$\frac{d}{dt}\left(\frac{u_u^2 h}{2}\right) = a_1 \epsilon L_m (= -F - D + M), \tag{22}$$

where F is the force responsible for changing the potential energy of the flow, D is the dissipation and M is the force applied on the upper layer for driving the fluid. a_1 is a scaling parameter.

$$\frac{d}{dt}\left(\frac{u_u^2 h}{2}\right) = 2\Gamma_u c_D \frac{L_m}{h}\frac{u_u^2}{2} u_u, \tag{23}$$

if $a_1 a_2 = \Gamma_u c_D$. From (21),

$$c_D \frac{L_m}{h} u_u = \frac{Ri_m}{2\Gamma_\rho}\frac{dh}{dt}, \tag{24}$$

$$\frac{d}{dt}\left(\frac{u_u^2 h}{2}\right) = \frac{u_u^2}{2}\frac{2\Gamma_u Ri_m}{2\Gamma_\rho}\frac{dh}{dt}. \tag{25}$$

Assume,

$$\frac{u_u^2}{2} = \frac{\Omega^2 R^2}{2}\left(\frac{h_0}{h}\right)^{2\alpha},$$

$$\left(1 - \frac{2Ri_m\Gamma_u}{2\Gamma_\rho}\right)\frac{u_u^2}{2}\frac{dh}{dt} - 2\alpha\frac{\Omega^2 R^2}{2}h_0^{2\alpha}hh^{-2\alpha-1}\frac{dh}{dt} = 0, \tag{26}$$

$$\left(1 - \frac{2Ri_m\Gamma_u}{2\Gamma_\rho}\right)\frac{u_u^2}{2}\frac{dh}{dt} - 2\alpha\frac{u_u^2}{2}\frac{dh}{dt} = 0, \tag{27}$$

$$\frac{Ri_m\Gamma_u}{\Gamma_\rho} = 1 - 2\alpha. \tag{28}$$

It has been found experimentally that $Ri_m = 0.2$ (see [3], [6]). Substituting $\alpha = 0.4$ (as suggested by figure 11(e)) along with $Ri_m = 0.2$, analysis reveals that

$$\Gamma_u \sim \Gamma_\rho.$$

This is an interesting result showing that for intermediate values of Ri_B, an equal amount of energy goes into driving the fluid and in mixing the layers.
Moreover, if $\alpha = 0, \Gamma_u = 5\Gamma_\rho$. Thus, for the solid body rotation case (small Ri_B), the proportion of energy that goes into driving the fluid is much larger than the proportion that is spent on mixing. On the other hand, if $\alpha = 0.5, \Gamma_u = 0$. As mentioned before, this represents the case where there is no change in the kinetic energy of the upper layer fluid. Thus, all the energy is spent on entraining the lower layer fluid.

6 Conclusion

It can be concluded from the above analysis and experimental work that a Ri_B^{-1} law for mixing is not found. Moreover, the fluid velocity in the upper layer is not always ΩR. It would appear that the upper layer is not always spun-up during the experiment and is not constant with h. It can be seen both from the theory and the density profiles that the height of the interface decreases with time. For moderate values of Richardson number, energy spent on mixing is of the same order as the energy that goes into mean velocity. For values of $Ri_B \geq 1$, the dynamics is completely different. The flow is no longer turbulent. This implies that the Reynolds number can play a significant role in determining the dynamics and can no longer be ignored. The qualitative behavior observed during an experiment at these values of Ri_B is very different than the observed behavior for lower values of Ri_B. The fluid is no longer mixed by eddies at the interface. The interface in this case is very thin and dominated by wave activity.

It is safe to say that the model developed here can capture the various aspects of mixing for $Ri_B \leq 1$. More work is required to understand the higher Richardson number cases.

7 Acknowledgements

This work was funded under the Geophysical Fluid Dynamics Summer Program at Woods Hole Oceanographic Institution. A special thanks to Colm Caulfield and Claudia Cenedese for the inspiration and guidance of this project. The many discussions with them were extremely valuable and helpful. Thanks to Neil Balmforth for directing the summer school and all the faculty members who came and made this summer school a very exciting place to learn about the many aspects of geophysical fluid dynamics.

References

[1] D. Boyer, P. Davies, and Y. Guo, *Mixing of a two-layer stratified fluid by a rotating disc.*, Fluid Dynamics Research, 21 (1997), pp. 381–401.

[2] P. Davies, Y. Guo, D. Boyer, and A. M. Folkard, *The flow generated by the rotation of a horizontal disk in a stratified fluid.*, Fluid Dynamics Research, 17 (1995), pp. 27–47.

[3] H. Fernando, *Turbulent mixing in stratified fluids.*, Annu. Rev. Fluid Mech., 23 (1991), pp. 455–493.

[4] H. Kato and O. Phillips, *On turbulent entrainment at a stable density interface.*, J. Fluid Mech., 37 (1969), pp. 643–655.

[5] T. Osborn, *Estimates of the local rate of vertical diffusion from dissipation measurements*, Journal of Physical Oceanography, 10 (1980), p. 8389.

[6] W. Peltier and C. Caulfield, *Mixing efficiency in stratified shear flows.*, Ann. Rev. Fluid Mech, 35 (2003), pp. 135–124.